BULLETIN OF THE EARTHQUAKE RESEARCH INSTITUTE
Vol. 43 (1965), pp. 349-379

23. *Deformation and Fracture of Rocks under Confining Pressure (2)*
Elasticity and Plasticity of Some Rocks.

By Kiyoo MOGI,

Earthquake Research Institute.

(Read Feb. 23, 1965.—Received Mar. 31, 1965.)

Abstract

Results of triaxial compression tests on ten dry rocks, including peridotite, diorite, granite, andesite, trachyte, tuff, and marble, are described and the pressure dependence of Young's modulus, plasticity, and strength are discussed.

With an improved strain measurement, the load and the deformation were accurately measured without any frictional error. The deformation curve was obtained with a constant strain rate, but at some stages of deformation the differential stress was reduced to zero and again increased. By this cyclic loading test, the permanent strain was separated from the elastic strain, and Young's modulus was obtained from the mean slope of the unloading or reloading curve. These rocks also showed remarkable elastic hysteresis. Young's modulus, permanent strain, and elastic hysteresis were obtained as functions of the compressional strain and the confining pressure. The transition from brittle fracture to ductile flow and the pressure dependence of strength are also discussed. According to these experimental results, the mechanical property of rocks under confining pressure seems to depend mainly on porosity besides mineral composition.

A preliminary experiment on the effect of previous loading is also described.

1. Introduction

A laboratory experiment on the mechanical behavior of rocks under confining pressure is carried out as a continuation of the preceding experiment. In many previous experiments[1)2)] including the preceding

1) E. C. ROBERTSON, "Experimental study of the strength of rocks," *Bull. Geol. Soc. Amer.*, **66** (1955), 1275-1314.

2) J. HANDIN and R. V. HARGER Jr., "Experimental deformation of rocks under confining pressure: Tests at room temperature on dry samples," *Bull. Assoc. Petrol. Geologists*, **41** (1957), 1-50.

one[3], the strain of rock specimen was measured indirectly from the displacements of the ram of the press, and stress-strain curves were derived by correcting these displacements for elastic distortion of the apparatus. This correction reduces the accuracy of strain measurement, and so the slope of the stress-strain curves has not been discussed quantitatively. In these studies, the breaking or yielding strength and the general feature of the large deformation have mainly been investigated. Recently, Brace[4] and Matsushima[5] successfully measured Young's modulus of compact brittle rocks under high confining pressure by use of the directly bonded electric resistance strain gages. The bonded strain gage is applicable for such comparatively small, homogeneous strain, but it does not follow large or heterogeneous deformation which usually appears in rock deformation under confining pressure.

In this experiment, the strain was obtained also with accuracy for large and heterogeneous deformations from the bending of thin steel plates connected to the ends of rock specimen. This bending of the plates was measured by bonded strain gage. Ten dry rocks including various rock types were tested by this method under confining pressures ranging from 1 to 2500 bars. From these precise stress-strain curves, the elastic modulus, the permanent strain in various stages of deformation, and the breaking or yielding strength were obtained as functions of confining pressure, and the transition from brittle fracture to ductile flow is discussed.

2. Experimental procedure

Ten dry rocks in Japan, about 60 specimens, were tested at room temperature by a conventional triaxial compression method. The experimental procedure is similar to that in the preceding test[6], except for the strain measurement. The test specimens were cylinders of 40mm diameter for six weaker rocks and 20mm diameter for three hard rocks, height-diameter ratio being nearly 2.0. The specimens were jacketed with soft rubber, Devcon Flexane 85, of 2mm wall thickness and thin

---

3) K. MOGI, "Deformation and fracture of rocks under confining pressure (1) Compression tests on dry rock sample," *Bull. Earthq. Res. Inst.*, **42** (1964), 491-514.

4) W. F. BRACE, "Brittle fracture of rocks," paper presented at Intern. Conf. on the State of Stress in the Earth's Crust, (1964), 110-178.

5) S. MATSUSHIMA, "On the flow and fracture of igneous rocks," *Disaster Prevent. Res. Inst. Bull.*, No. **36** (1960), 1-9.

6) K. MOGI, *loc., cit.*, 3).

polyvinyl sheet attached to the hard steel end pieces which were connected to rock specimens. The testing apparatus at Waseda University, described in the preceding paper, was also used in this experiment. The axial stress was applied by a hydraulic testing machine. The confining pressure was supplied independently by another oil compressor. The value of confining pressure is indicated by a Boudon gage. The axial load was measured by a load gage situated between a steel end

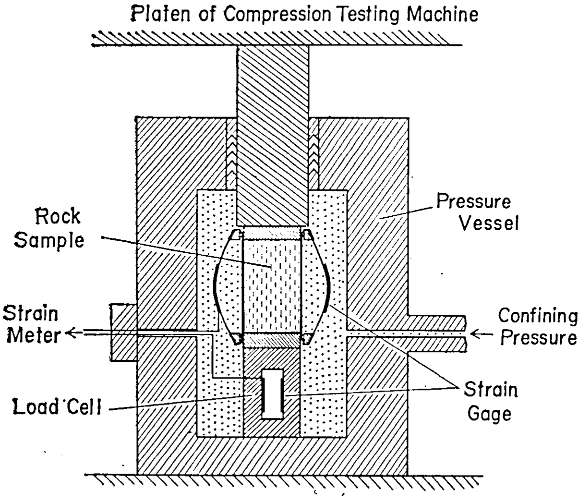

Fig. 1. Schematic view of apparatus.

piece fixed to the test specimen and the bottom of the pressure vessel. The load gage, a closed hollow steel cylinder with an electric resistance strain gage bonded on the inside of the cylinder, indicates the axial load without any frictional error.

The strain measurement was improved in this experiment. The dial gage method in which the strain is obtained from the displacement of the piston of the press, is not accurate enough for a precise analysis of the stress-strain curve and it is not applicable for cyclic loading because this system shows a remarkable hysteresis. The electric resistance strain gage bonded directly on the surface of specimen is frequently used for strain measurement of rock specimens at atmospheric pressure and it is also applicable for compact brittle rocks under high confining pressure. Although this method is highly sensitive and applicable to a cyclic loading test[7], the gage does not measure large deformations and give the true mean strain in heterogeneous deforma-

7) W. F. BRACE, *loc. cit.*, 4).

tions including microcracks, faults, etc. The present improved method shown in Fig. 1 is successfully applied to small and/or large deformations and also to heterogeneous deformations. A pair of thin steel plates is fixed to the upper and lower steel end pieces connected to the rock specimen, and shortening of the rock cylinder causes the bending of the thin plates. The bending deformation of the plate is measured by the bonded strain gages. As the elastic distortion of steel end pieces is generally negligible for its small thickness, the strain gage output indicates the axial displacement by a suitable calibration. The sensitivity of this method is adjusted by selecting the thickness of the thin plates. Since this system of the strain measurement does not show any appreciable hysteresis for loading and unloading, this method is applicable for cyclic loadings. There is another problem. The strain gage behavior under pressure should be considered in this study, because the bonded strain gage shows a remarkable "pressure effect" due to hydrostatic pressure[8]. However, the change in strain under constant hydrostatic pressure is measured similarly to the atmospheric case. Figure 2 is an experimental result showing this. Strains (A) and (B) are the axial strains of the outside and inside respectively of the hollow steel cylinder with closed ends under axial compression. Curve I is in atmospheric pressure and Curve II is in 2000 bars confining pressure, and these two curves are nearly similar. Thus, the hydrostatic pressure does not appreciably affect the gage factor.

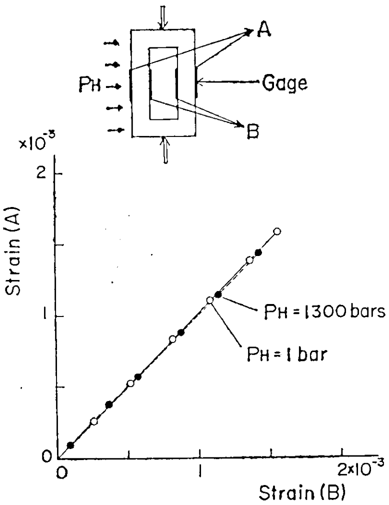

Fig. 2.

In this method, the strain gage output is not a linear function of the true strain. The calibration of gage output is troublesome and reduces more or less the accuracy of strain measurement. This should be improved in future.

Thus, the precise stress-strain relations were obtained for elastic and plastic stages of various rocks. The load was applied at a nearly constant strain rate of 0.15~0.2 percent per min. The differential

8) W. F. BRACE, "Effect of pressure on electric resistance strain gages," *Exp. Mech.*, 4 (1964), 212-216.

stress was reduced to zero at various stages of deformation, the elastic and permanent strains being obtained at each stage.

3. Stress-strain relation

Tested rocks are a peridotite, a diorite, a granite (strength only), two andesites, a trachyte, three tuffs and a marble (Appendix). Their density and porosity are tabulated in Table 1. Some of the rocks which were tested in the preceding experiment were also studied in the present one, but these rock samples in both cases are from different blocks of the same rocks.

The test specimens were compressed to breaking for very brittle rocks and to 3∼4 percent strain for ductile rocks, and at various stages of deformation the stress was reduced to zero or very small

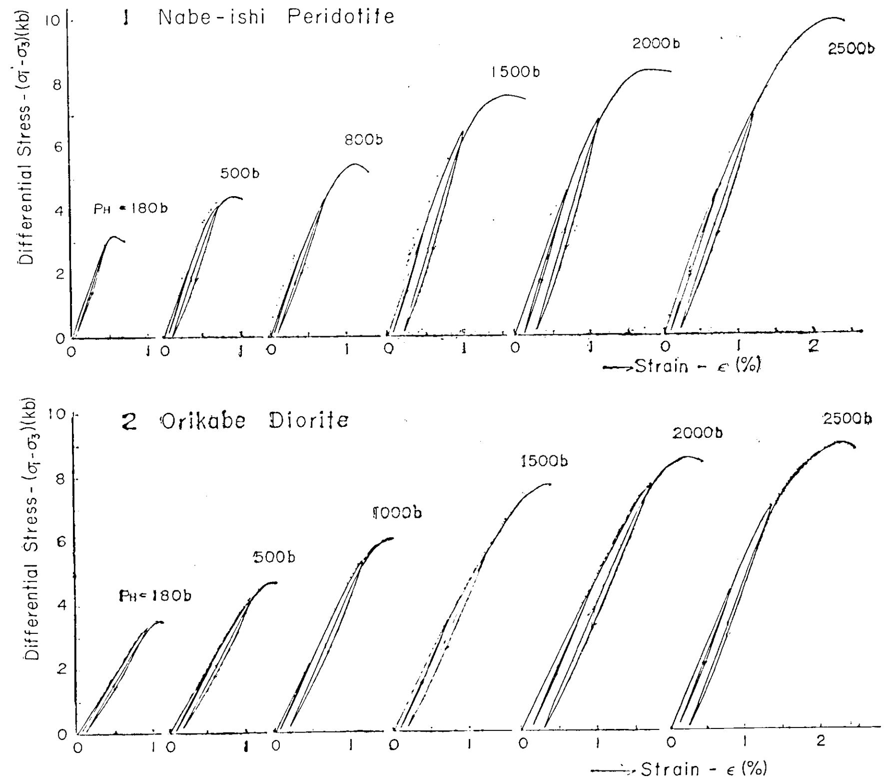

Fig. 3. (a) Stress-strain curves in compression at room temperature. Confining pressure in bars given for each curve.

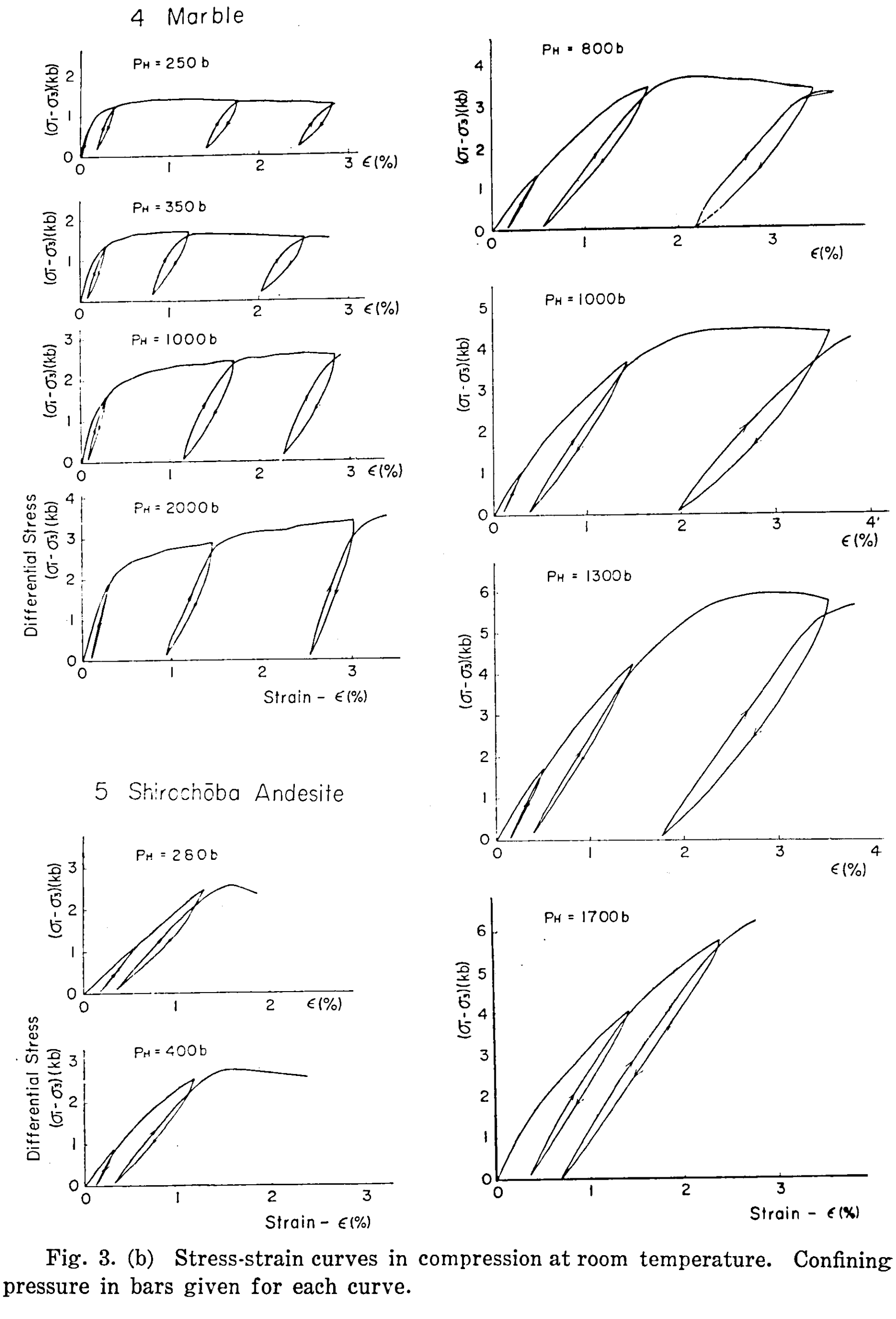

Fig. 3. (b) Stress-strain curves in compression at room temperature. Confining pressure in bars given for each curve.

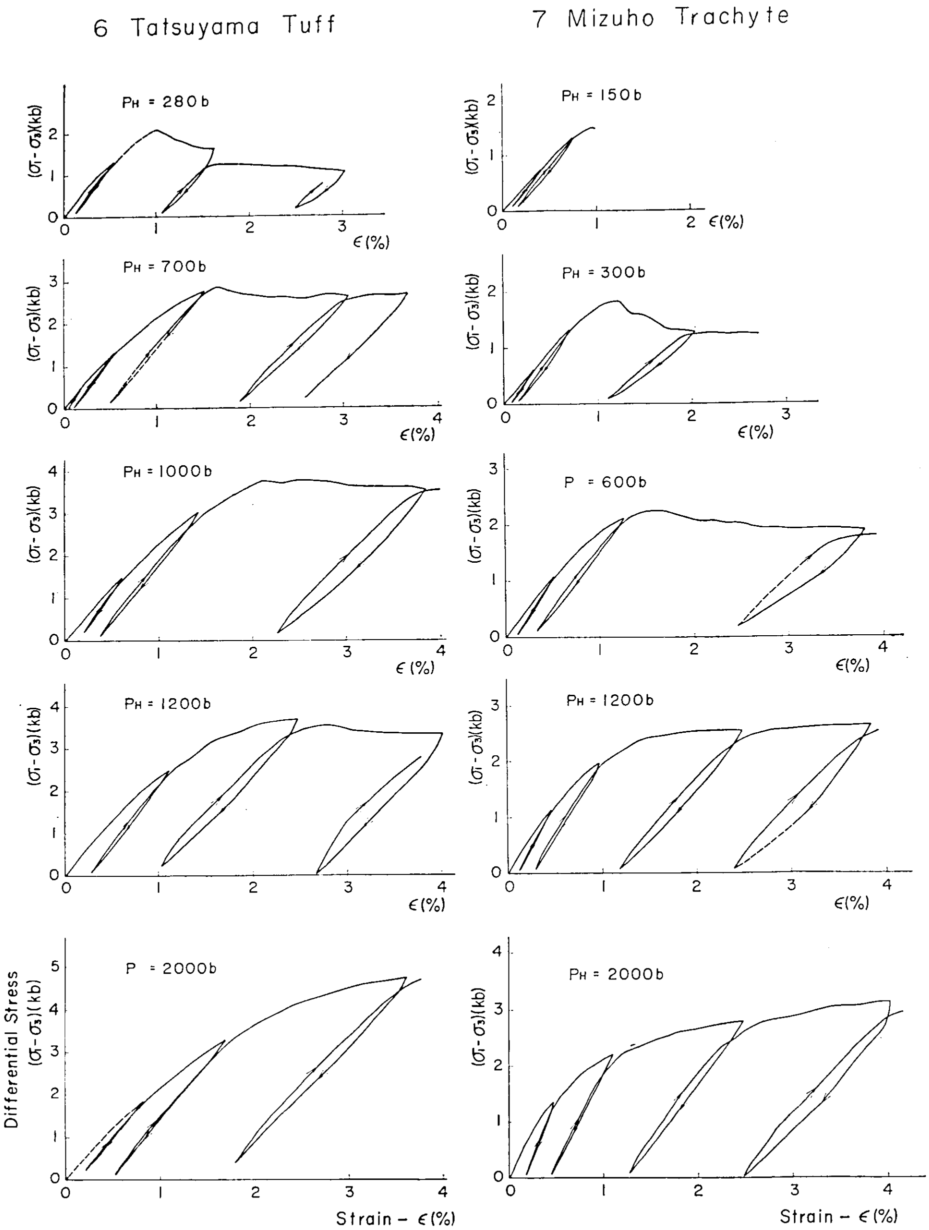

Fig. 3. (c) Stress-strain curves in compression at room temperature. Confining pressure in bars given for each curve.

Table 1. Density and porosity of tested rocks.

No.	Rock	Bulk density (g/cc)	Porosity (%)
1	Nabe-ishi peridotite	3.16	0.02
2	Orikabe diorite	2.78	0.4
3	Mannari granite	2.62	0.7
4	Mito marble	2.69	0.2
5	Shirochōba andesite	2.45	5.1
6	Tatsuyama tuff	2.26	10.2
7	Mizuho trachyte	2.24	8.5
8	Shinkomatsu andesite	2.17	12.6
9	Ao-ishi tuff	2.01	17.3
10	Saku-ishi welded tuff	1.95	21.6

values, then increased again. The stress-strain curves in reloading are frequently different from a virgin stress-strain curve and the permanent strain remains at zero stress.

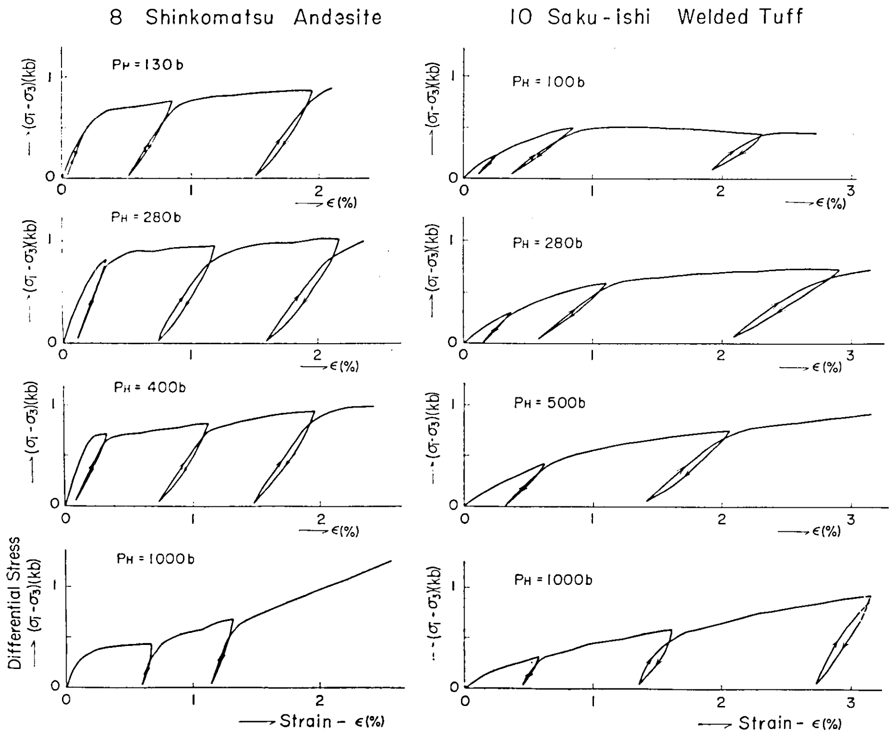

Fig. 3. (d) Stress-strain curves in compression at room temperature. Confining pressure in bars given for each curve.

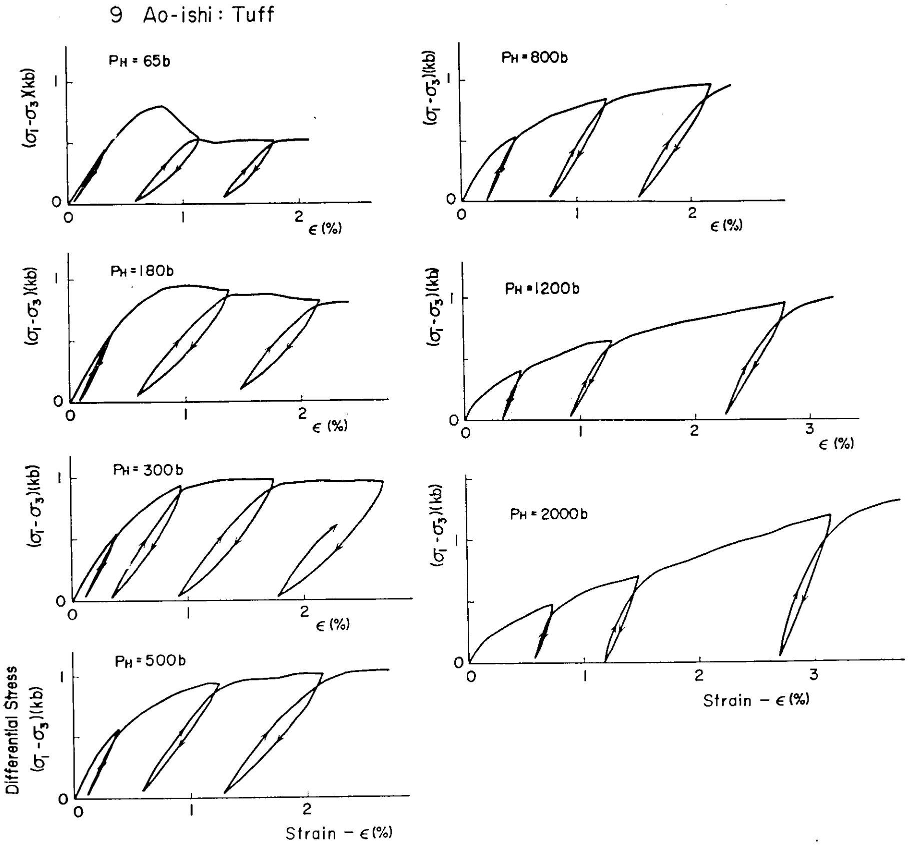

Fig. 3. (e) Stress-strain curves in compression at room temperature. Confining pressure in bars given for each curve.

Stress-strain curves in compression for different values of the confining pressure are shown in Fig. 3. The stress is the maximum difference of principal stresses, which is equal to twice the maximum shear stress. In all cases, the stress calculation is based on the initial cross-sectional area, because the deformation is not so large ($\lesssim 4$ percent).

The experimental results are consistent with many previous investigations, that is, igneous compact rocks are very brittle and become remarkably stronger, as the confining pressure is raised while other porous rocks become plastic. However, the precise feature of these curves suggests complex processes of deformation. For example, the initial part of deformation before yielding, the so-called *elastic part*, is appreciably curved and includes remarkable permanent deformation in many cases. The slopes of these stress-strain curves are different from the elastic modulus in this stage.

The terms *brittle* and *ductile* are frequently used in the present discussion. Here, their definitions are given as follows. The brittle behavior is characterized by a sudden change of slope in the stress-strain curve at the yield point followed by a complete loss of cohesion or an appreciable drop in differential stress. The ductile behavior is characterized by the deformation without any downward breaks in slope after the yield point. Some discussion on the difinition of *brittle, ductile,* and *yielding* will be given in a later section.

4. Modulus of elasticity

When the rock specimen is unloaded to zero differential stress, after it is compressed to a point P in Fig. 4 and then reloaded, the branches (P2Q, Q3P) are different from the virgin loading curve (O1P) in many cases, as shown in Fig. 4. The unloading and reloading curves usually differ little from each other and form a narrow loop (P2Q3). The reloading curve (Q34) passes very near to the point P from which the unloading branch drops down and thereafter continues to the virgin loading curve (O1P). This narrow loop circumscribed by the unloading and reloading branches may be approximately substituted by a straight line $\overline{PQ}$. The slope of this line is taken as the mean Young's modulus.

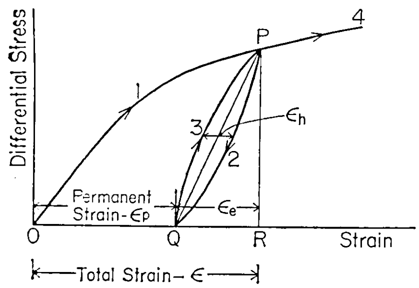

Fig. 4. Typical stress-strain curve.

Figure 5 shows the relation between Young's modulus and the strain at the point (P) for different values of confining pressure. According to the result, Young's modulus differs considerably at various stages of deformation. In compact igneous rocks, Young's modulus is nearly constant before fracture. In other porous rocks, it sometimes does not vary, sometimes decreases to some degree before breaking or yielding. According to results by dynamic method[9], the modulus may increase at an initial stage with the increase of stress, but this stage was not

9) S. MATSUSHIMA, "Variation of the elastic wave velocities of rocks, in the process of deformation and fracture under high pressure," *Disaster Prevent. Res. Inst. Bull.*, No. **32** (1960), 1-8.

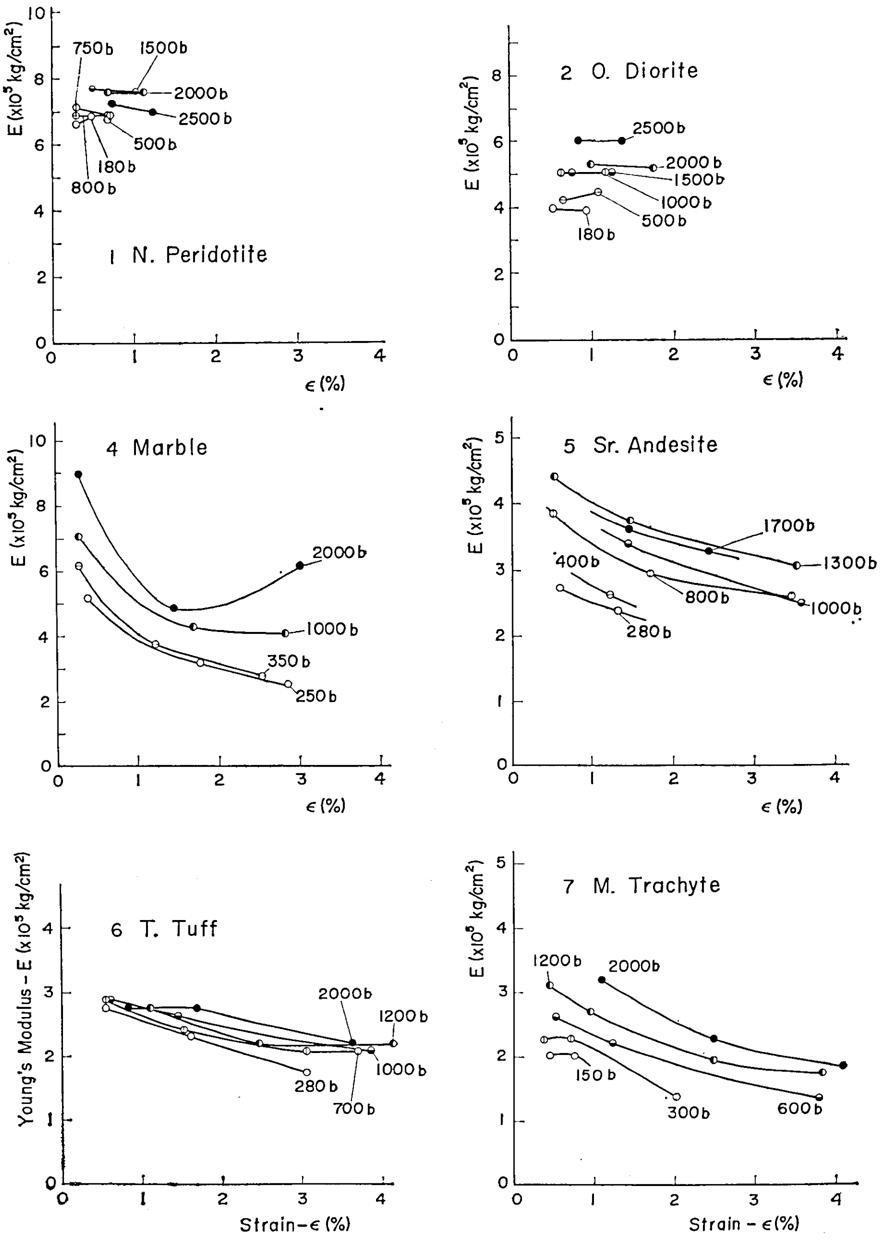

Fig. 5. (a) Relation between Young's modulus and the compressional strain. Confining pressure in bars given for each curve.

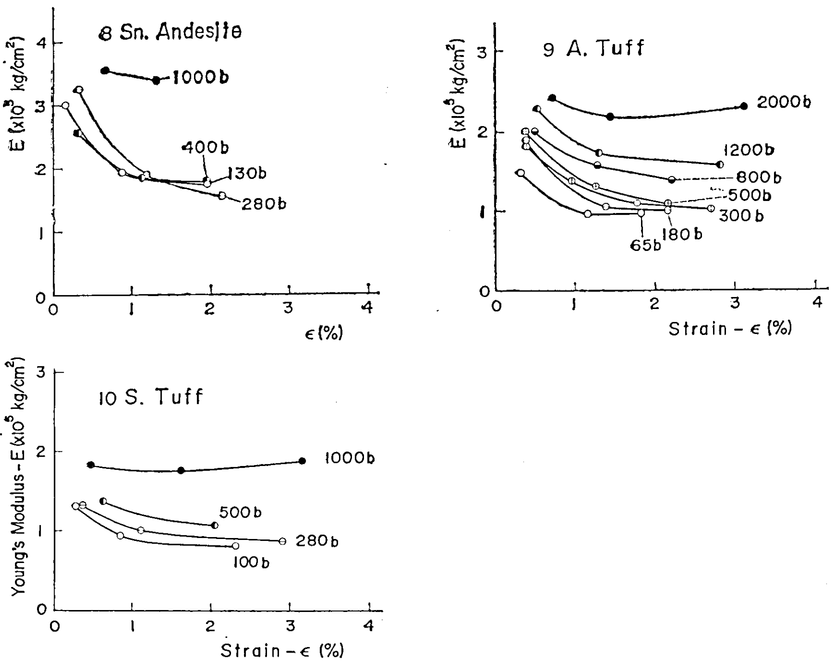

Fig. 5. (b) Relation between Young's modulus and the compressional strain. Confining pressure in bars given for each curve.

investigated in the present experiment. After the breaking or yielding the modulus of elasticity decreases remarkably, especially under lower pressure. The modulus of ductile rocks (tuffs and a marble) under higher pressure decreases slightly just after the yield point and begins to increase with compressional strain.

These results give a suggestion on the mechanism of deformation of rocks. That is, the structure does not vary remarkably before yielding and is considerably fractured after yielding. This result suggests that yielding of rocks may be caused by internal micro-fracturing besides dislocation. Under lower pressure, the straining after yielding causes more fracture of structure. On the other hand, the straining of ductile rocks under higher pressure strengthens the structure by compaction.

The relations between Young's modulus and the confining pressure for different values of the strain at point (P) are shown in Fig. 6. The graphs were drawn from the above-mentioned relation between Young's modulus and the strain by interpolation of Young's modulus. The modulus increases more or less with pressure. The modulus of Nabe-ishi peridotite is largest in the present test and slightly increases with

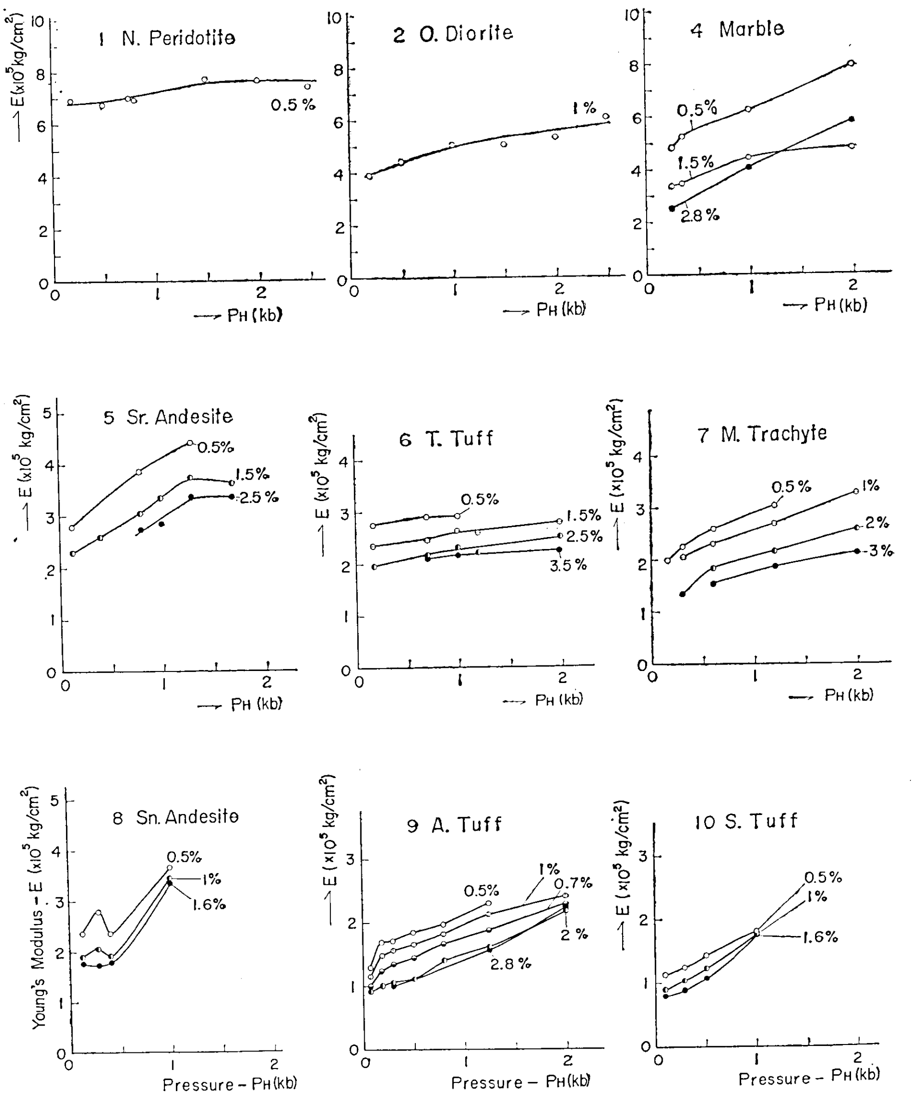

Fig. 6. Relation between Young's modulus and the confining pressure. Strain in percent given for each curve.

pressure. The modulus of Orikabe diorite is lower than Nabe-ishi and its increase is more appreciable. These results on igneous compact rocks are consistent with similar results by Brace[10], and with results on

10) W. F. BRACE, *loc. cit.*, 4).

elastic wave velocity[11]. In more porous rocks, Young's modulus increases more remarkably with the confining pressure.

The pressure dependence of Young's modulus in Shinkomatsu andesite is abnormal in lower pressures. Young's modulus increases to 280 bars and drops noticeably at 400 bars. This drop of Young's modulus is not so clear at larger strains. As seen in a later section, its strength also begins to decrease at pressures between 280 and 400 bars. This abnormal change in Young's modulus seems to be attributed to the mechanical structure of these rocks. That is, most of the pores in this volcanic rock (porosity: 12.6 percent) are isolated round holes in a continuous framework, while porous sedimentary rocks have wedge-like openings between grains. The above-mentioned change seems to be due to fracturing of the framework by the confining pressure.

5. Elastic hysteresis

As mentioned above, the unloading and reloading curves form a narrow closed loop. Then, the reloading curve (Q34 in Fig. 4) passes near point P, the branch P4 being continuous to the loading curve O1P. In this case, the area of hysteresis loop indicates a heat loss due to a cyclic loading. A ratio h of this dissipative energy to the energy worked by elastic deformation is related to the viscosity of rocks. In this paper, $(\varepsilon_h/\varepsilon_e)\times 100$ percent is taken as an approximate value of h. ε_h is the maximum width in strain of the hysteresis loop and ε_e is the elastic strain by unloading or reloading.

Figure 7 shows the relation between h and the strain ε at the point P for different values of confining pressure and the relation between h and the confining pressure. The accuracy of the h value is not so high, but remarkable changes were observed. In compact igneous rocks, h increases slightly with deformation, but its value is small (<10 percent). In other silicate rocks, h is also small before breaking or yielding and increases appreciably after yielding. The h value slightly decreases with the increase of the confining pressure in these cases. Mito marble shows remarkable hysteresis in a cyclic loading, especially under lower confining pressure. The h value decreases considerably with the increase of the pressure. The increase of h after breaking or yielding may indicate the increase of the viscosity by internal

11) F. BIRCH, "The velocity of compressional waves in rocks to 10 kilobars, part I," *Jour. Geophys. Res.*, **65** (1960), 1083-1102.

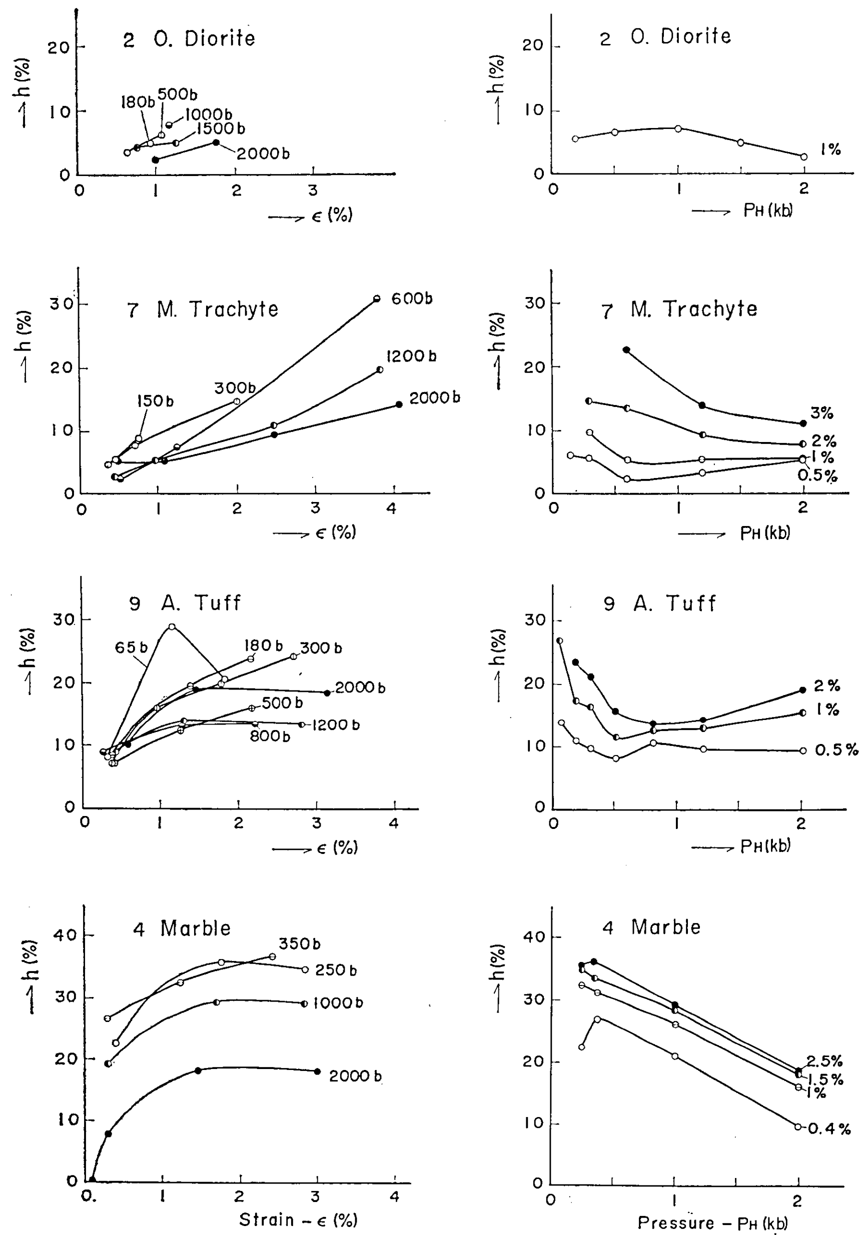

Fig. 7. Ratio of the dissipative energy due to elastic hysteresis to the energy worked by elastic deformation as functions of the strain and the confining pressure.

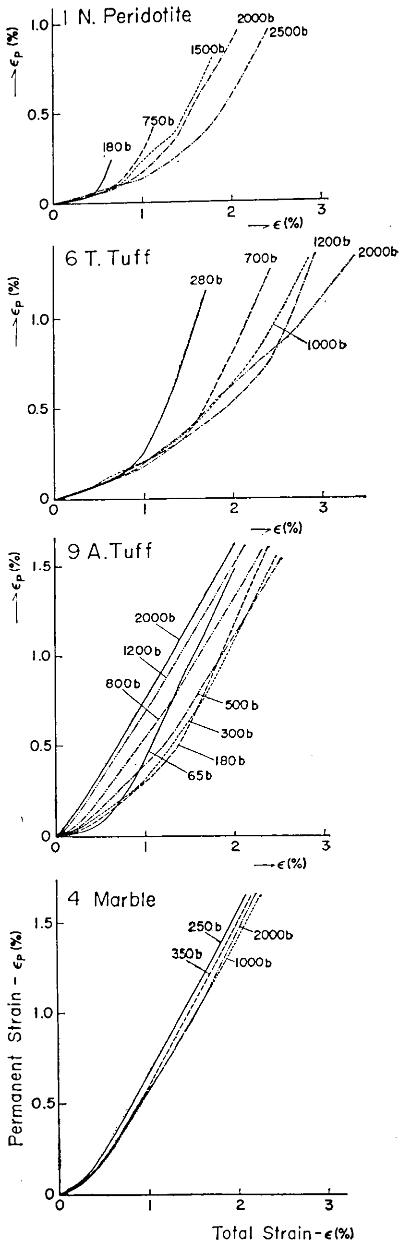

Fig. 8. Relation between the permanent strain and the total strain. Confining pressure in bars given for each curve.

micro-fracturing of specimen.

6. Permanent strain

The strain of the stressed rock is partly elastic and partly permanent. The elastic strain is obtained as a recovered deformation by unloading to zero stress and the permanent strain is also obtained as an unrecovered deformation (Fig. 4). This permanent strain includes various types of unrecoverable deformation due to dislocation, viscous flow, micro-fracturing, etc. and so it increases in some degree with the decrease of strain rate[12]. In this experiment, the permanent strain at various stages of deformation was obtained from deformation curves of strain rate (0.15~0.2) percent per min.

Figure 8 shows the relation between the total strain and the permanent strain at each stage for different values of the confining pressure. It is very noticeable that the permanent strain is found even at an initial stage of deformation in most rocks. In compact igneous rocks, which are the most brittle rocks, the permanent strain appears slightly in the linear part of stress-strain curve and increases abruptly from a proportional limit. The ultimate permanent strain increases considerably with the confining pressure. In some rocks of medium

12) H. C. HEARD, "The effect of large changes in strain rate in the experimental deformation of rocks," *Jour. Geol.*, **71** (1963), 162–195.

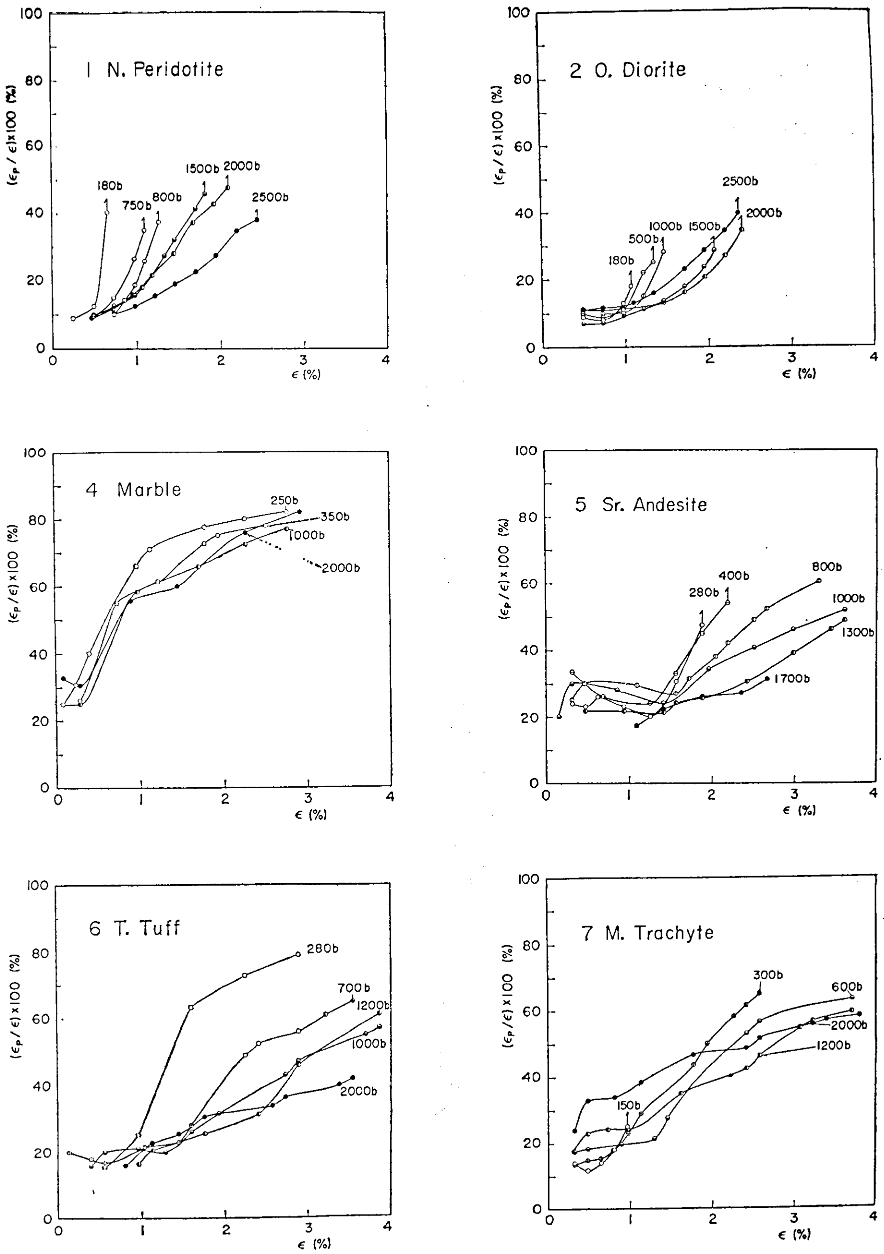

Fig. 9. (a) Relation between the ratio of the permanent strain to the total strain and the total strain. Confining pressure in bars given for each curve.

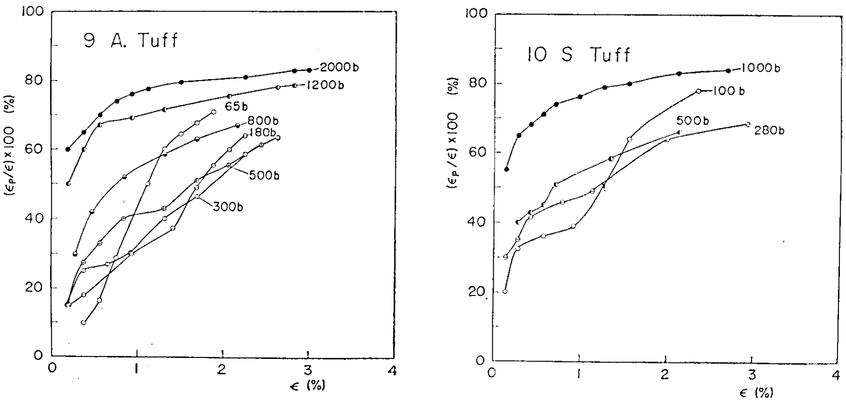

Fig. 9. (b) Relation between the ratio of the permanent strain to the total strain and the total strain. Confining pressure in bars given for each curve.

porosity, the appreciable permanent deformation increases linearly at the initial stage and the slope of this curve suddenly increases at some stages. The permanent strain in highly porous rocks is very large and increases continuously without any such sudden change in curve slope under high pressure. This point at which the slope of curves changes remarkably corresponds to the yield point which will be discussed in a later section. The value of the permanent strain at the yield point varies in a wide range from 0.1 to 1 percent strain and has no relation with fracturing behavior (Fig. 14).

The ratio of the permanent strain to the total strain is shown in Fig. 9, as a function of the total strain in different values of the confining pressure. The above-mentioned process of changes in the permanent strain is clearly observed, especially in the initial stage of deformation. The types of curves seem to have a close relation with the types of fracturing behavior, brittle or ductile (Fig. 10). That is, in brittle rocks including transitional ones, the ratio of the permanent strain to the total strain is smaller and nearly constant to middle stages of deformation, thereafter increasing remarkably. On the other hand, this ratio in ductile rocks is larger even at an initial stage and increases remarkably, but the increasing rate decreases in later stages. As shown in Fig. 14, the $\varepsilon_p/\varepsilon$ value at yield point seems to be smaller in brittle cases than in ductile ones.

The relation of the $\varepsilon_p/\varepsilon$ value to the confining pressure is shown in Fig. 11. Here, it is noticed that there are the following two types in these curves. The one is the type in which the ratio is independent of

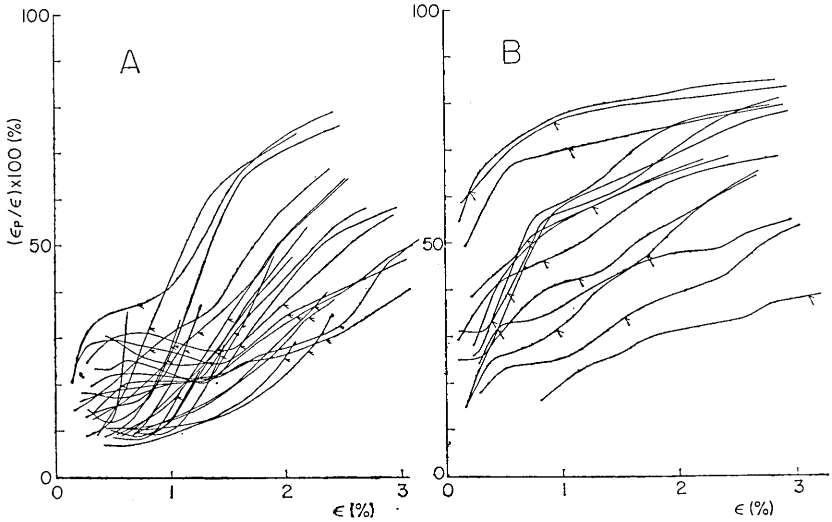

Fig. 10. Relations between the ratio of the permanent strain to the total strain. A: brittle state, B: ductile state. Arrow indicates the yield point.

the pressure, especially at an initial stage of deformation (<1 percent strain). The rocks having smaller porosity belong to this type. The other type is seen in very porous rocks, such as A. tuff and S. tuff. In this case, the ratio $\varepsilon_p/\varepsilon$ increases remarkably with the confining pressure.

7. Relation between strength and confining pressure

The brittle fracture and the ductile flow were defined in Section 3. Strength in the brittle state is the maximum stress achieved during an experiment. This value is definitely determined. However, strength in the ductile state, namely yield stress, is usually indefinite. Generally, the yield stress is the stress at which the sudden transition from the elastic to the plastic stage takes place, and so the stress at the knee of the stress-strain curves or the stress at the proportional limit is taken as the yield stress[13]. In some rocks, the knee of the stress-strain curve is clear and the usual definition is applicable. However, other rocks show a gradual transition from elastic to plastic stage, and so it is indefinite because of the lack of a marked break in the curve. Then, the slope of the stress-strain curve varies frequently even at initial stages of

13) E. C. Robertson, *loc. cit.*, 1).

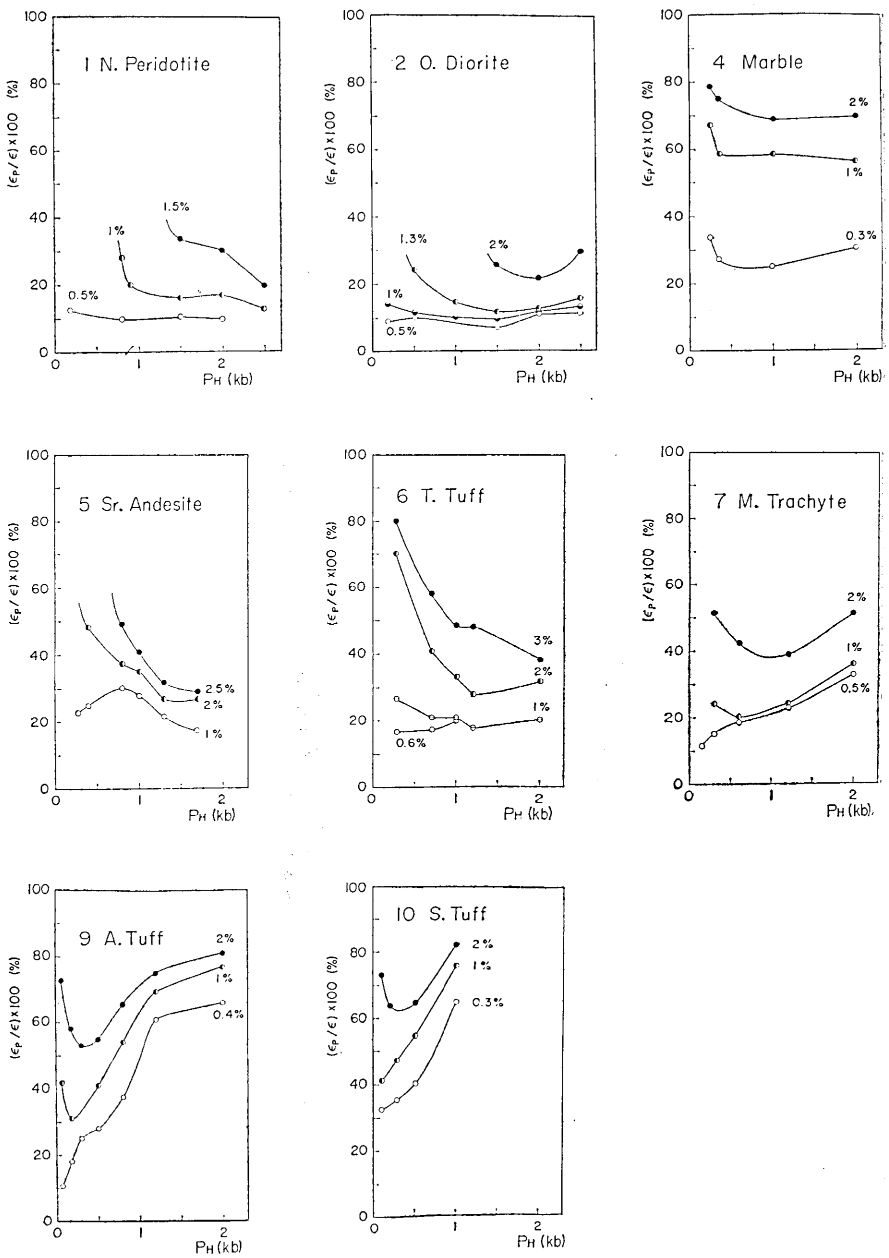

Fig. 11. Relation between the ratio of the permanent strain to the total strain and the confining pressure. Strain in percent given for each curve.

deformation, and so the curve has no proportional limit. Sometimes the yield point is also defined as a point having an appreciable limit value of permanent deformation. This definition is also not always suitable for rocks, because the value of the permanent strain at the marked

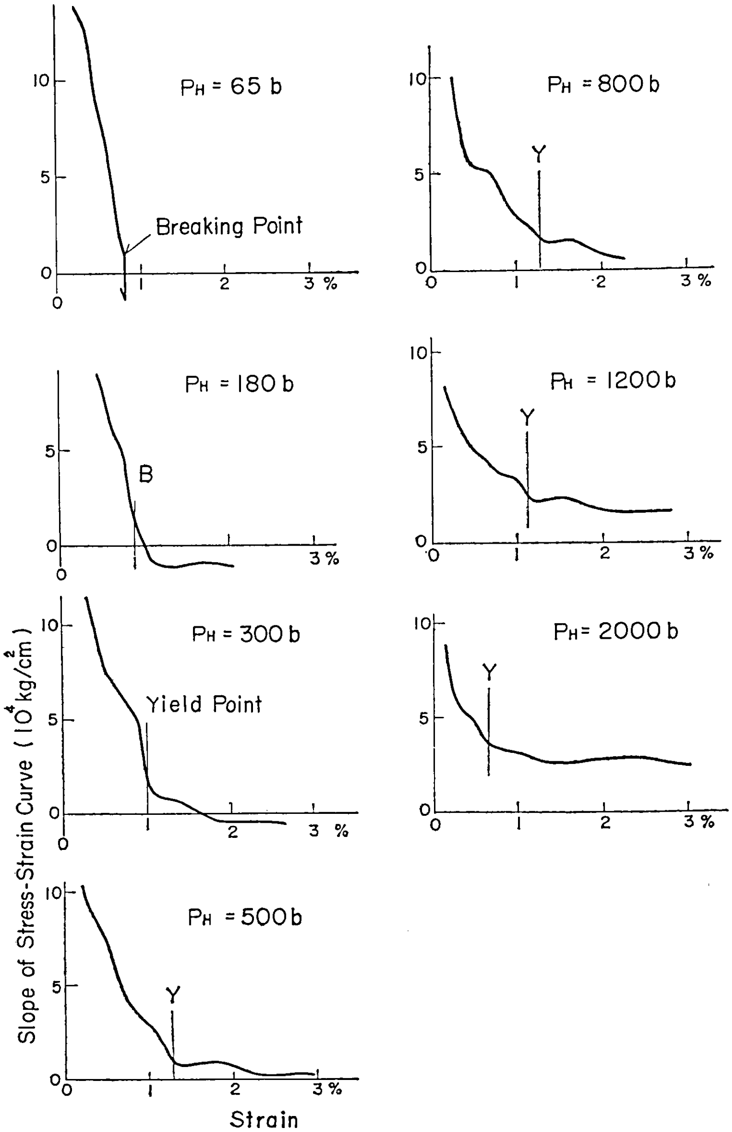

Fig. 12. Relation between $\frac{\partial(\sigma_1-\sigma_3)}{\partial\varepsilon}$ and ε in Ao-ishi tuff. Confining pressure in bars given for each curve.

Table 2. Strength and behavior of rocks.

Rock	Confining pressure (bars)	Strength (bars)	Behavior
1. Nabe-ishi peridotite	180	3170	brittle
	500	4440	brittle
	750	5170	brittle
	800	5440	brittle
	1000	6070	brittle
	1300	6810	brittle
	1500	7590	brittle
	1600	8090	brittle
	2000	8380	brittle
	2500	9940	brittle
2. Orikabe diorite	180	3530	brittle
	500	4710	brittle
	1000	6060	brittle
	1500	7700	brittle
	2000	8530	brittle
	2500	8940	brittle
3. Mannari granite	180	3860	brittle
	280	4360	brittle
	600	5700	brittle
	1000	7410	brittle
	1800	9300	brittle
	2200	9600	brittle
4. Mito marble	150	930	transitional
	250	1140	transitional
	350	1490	ductile
	1000	1960	ductile
	2000	2430	ductile
5. Shirochōba andesite	280	2500	brittle
	400	2750	brittle
	800	3650	transitional
	1000	4330	transitional
	1300	5730	transitional
6. Tatsuyama tuff	280	2070	brittle
	400	2370	brittle
	700	2870	brittle
	1000	8750	transitional
	1200	3630	transitional
	2000	4270	ductile
7. Mizuho trachyte	150	1490	brittle
	300	1870	brittle
	600	2230	transitional
	1200	2420	ductile
	2000	2610	ductile
8. Shinkomatsu andesite	130	635	ductile
	280	840	ductile
	400	697	ductile
	1000	384	ductile
9. Ao-ishi tuff	65	786	brittle
	180	930	brittle
	300	947	ductile
	500	940	ductile
	800	846	ductile
	1200	625	ductile
	2000	460	ductile
10. Saku-ishi welded tuff	100	500	transitional
	280	528	ductile
	500	456	ductile
	1000	?	ductile

break of the stress-strain curve is not constant and varies in a wide range. Therefore, the yielding in the usual sense is seen only in some rocks under certain conditions.

If the yielding is used in a wide sense, the yield stress of rocks may be more generally defined in the following way. The local yielding begins to take place even under very low stress, because the stress in the specimen having ununiform structures distributes concentratively around structural irregular points. Thus, the yielding in such ununiform materials gradually takes place in a wide range of stress value, but this yielding may be completed at a certain stress value. This terminal stress is taken as yield stress. In fact, the slope of the stress-strain curve decreases with the increase of stress and becomes nearly constant at this yield stress in many cases. This definition is consistent with the above-mentioned usual definition in the case having a marked break of the stress-strain curve. Figure 12 shows the relation between $\partial\sigma/\partial\varepsilon$ and ε in Ao-ishi tuff. In a ductile state, the point at which $\partial\sigma/\partial\varepsilon$ becomes nearly constant is taken as the yield point. Vertical lines indicate the breaking or the yielding. In this paper, the yield stress in such a wide sense is discussed.

The strength of each rock specimen is summarized in Table 2. Figure 13 shows the relation between the strength and the confining pressure. In this figure, closed circles indicate the breaking strength and open circles the yield strength. Then, semi-closed circles indicate the transitional case in which the slope of the stress-strain curve after yielding slightly drops. These strength-

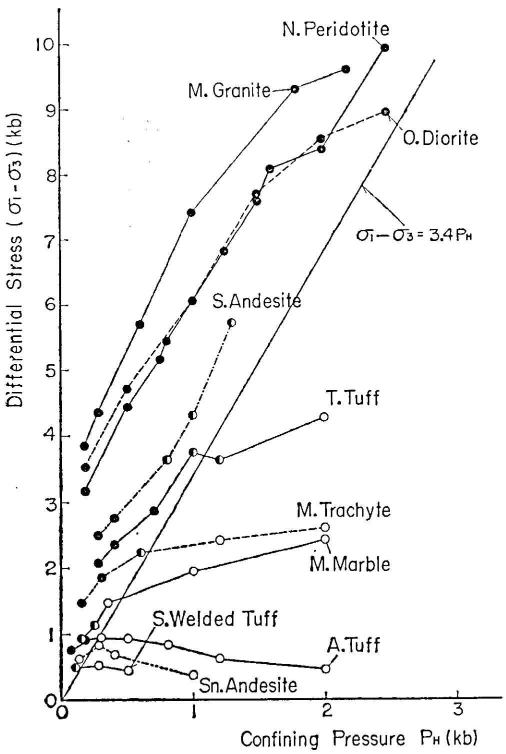

Fig. 13. Relation between the compressive strength and the confining pressure. closed circle: brittle; open circle: ductile; semi-closed circle: transitional.

pressure relations may be classified into the following three groups.

(1) Igneous compact rocks (peridotite, diorite, granite) are strongest and always brittle in the range of confining pressure from 1 to 2500 bars. The slope of the curve is largest among the present tested rocks and decreases gradually with the increasing pressure, except for Nabe-ishi peridotite.

(2) Three rocks (Shirochōba andesite, Tatsuyama tuff, and Mizuho trachyte) of medium porosity ($5\sim10$ percent) have intermediate strengths. The behavior is brittle under lower pressure and ductile under higher pressure, and frequently transitional under intermediate pressure. The slope of the strength-pressure curve is larger under lower pressure and decreases remarkably at high pressure, but it is positive. The pressure dependence of strength in Mito marble belongs to this type.

(3) The three very porous rocks (Ao-ishi tuff, Saku-ishi tuff, Shin-komatsu andesite) are weakest and remarkably ductile, except for very low pressures. The strength slightly increases with the pressure under lower pressure, but decreases appreciably with the increasing pressure under moderate pressure.

Furthermore, it is very interesting that the brittle region in this figure is separated from the ductile region by a line. According to a recent investigation, this boundary line is nearly expressed by

$$\sigma_1-\sigma_3=3.4\,P_H.$$

This line is also represented in the figure. In general, the slope of the strength-pressure curve is large in the brittle region and small in a positive or negative value in the ductile region, the transition from brittle to ductile behavior seeming to take place gradually near the boundary line.

It is probable that such brittle-ductile transition may have a relation to the value of permanent strain at breaking or yielding. Figure 14 (a) shows the relation between the permanent strain at breaking or yielding and the confining pressure in various rocks. In this figure, closed circles are brittle, open circles ductile and semi-closed circles transitional. There seems to be no significant relation between the permanent strain and the brittle or ductile behavior. However, if the value of permanent strain is substituted by the ratio of the permanent strain to the total strain, a remarkable relation between them is revealed, as shown in Fig. 14(b). That is, a brittle region in this figure is separated from a ductile region nearly by a line. This boundary line is nearly parallel to the pressure axis. In another words, when the ratio exceeds the limit value (about 30～35 percent), the type of fracture becomes ductile. This fact gives a suggestion of the mechanism of the brittle-ductile transition. This problem will be discussed in another paper.

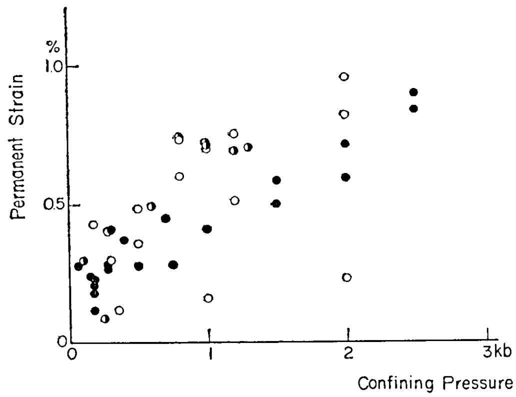

Fig. 14. (a) Relation between the permanent strain at breaking or yielding point and the confining pressure.

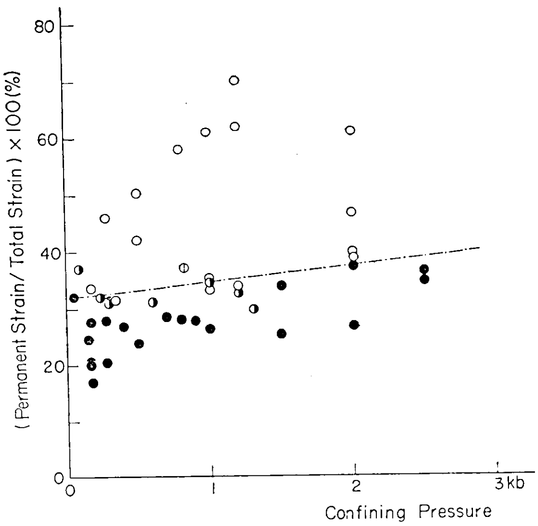

Fig. 14. (b) Relation between the ratio of the permanent strain to the total strain and the confining pressure.
closed circle: brittle; open circle: ductile; semi-closed circle: transitional.

8. Effects of previous loading

As mentioned above, rocks are not completely elastic materials, but they show remarkable plasticity. Therefore, the stress-strain relation is affected by a history of deformation before an experiment. If the effect of previous deformations is clarified, a history of deformation of rocks may be deduced from the present mechanical property. Here, as a preliminary step from this viewpoint, an effect of previous loading in Ao-ishi tuff was measured in some simple cases.

(1) *Hydrostatic pressure*

An effect of previously applied hydrostatic pressure was studied. Ao-ishi tuff specimens were previously exposed to the hydrostatic pressure of 800 bars and 2000 bars. Thereafter, these specimens were tested by compression under 180 bars confining pressure. Curves (B) and (C) in Fig. 15 show their stress-strain curves, compared with that of a virgin specimen (A). Relations of Young's modulus and the ratio of the permanent strain to the total strain to the compressive strain are shown in Fig. 16. The hydrostatic pressure of 800 bars applied previously increases slightly both the compressive strength and Young's modulus. On the other hand, 2000 bars hydrostatic pressure reduces remarkably both the strength and Young's modulus. The ratio of the permanent to the total strain at the breaking or yielding point is 20 percent in case (B) and 33 percent in case (C). The fracture behavior is brittle in (B) and ductile in (C). From the experimental result, it is deduced that this rock has not been buried in a larger depth than several kilometers.

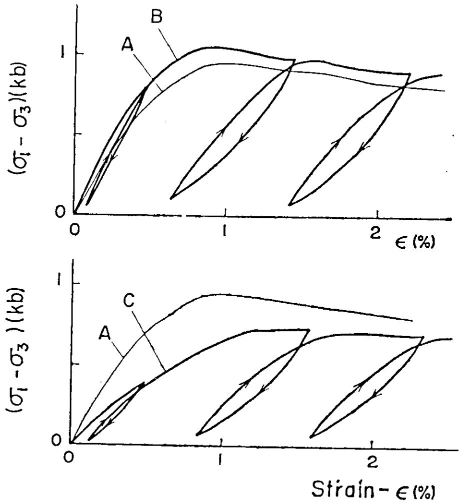

Fig. 15. Stress-strain curves of Ao-ishi tuff under 180 bars confining pressure. (A): virgin specimen; (B): Specimen previously exposed to 800 bars hydrostatic pressure; (C): to 2000 bars hydrostatic pressure.

(2) *Axial compression*

As seen in stress-strain curves by cyclic loading, Young's modulus and plasticity are affected by a previous compressional

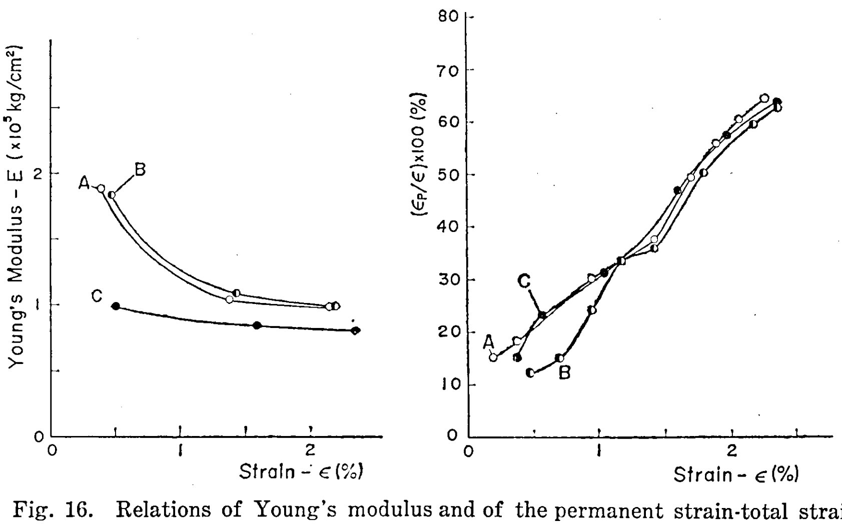

Fig. 16. Relations of Young's modulus and of the permanent strain-total strain ratio to the compressive strain, for (A), (B), and (C).

deformation. By previous compression, the knee of the stress-strain curve at yield point becomes marked and the yield strength increases or decreases by strain hardening or softening. In this experiment, only one case was measured. An Ao-ishi specimen was shortened by 2.2 percent by axial compression under 800 bars confining pressure. After being left for 18 hours at atmospheric pressure, the specimen was tested again by compression under 800 bars confining pressure (Fig. 17). Young's modulus decreases remarkably by previous loading, but its value corresponds to that in deformation continued without such intermission of loading. The stress-strain curve before yielding is nearly linear and the permanent strain in this stage is smaller as compared with the initial part of the virgin deformation. However, the permanent strain in this reloading increases remarkably by intermission of loading.

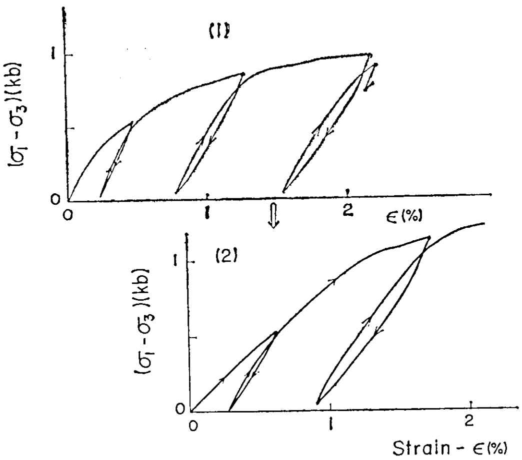

Fig. 17. (2): Stress-strain curve of Ao-ishi tuff under 800 bars confining pressure, after 2.2 percent shortening by previous compression. (1): curve of previous axial compression.

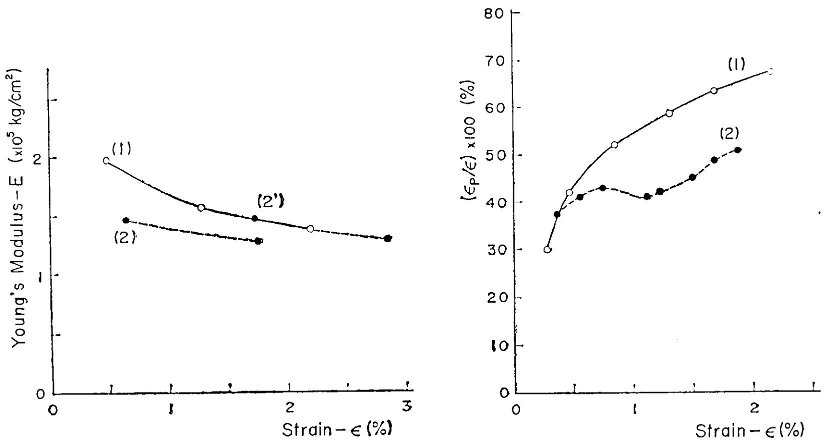

Fig. 18. Relations of Young's modulus and of the permanent strain-total strain ratio to the compressive strain, for (1) and (2).

Effects of previous loading may be very complex. However, a history of deformation is more or less reserved in mechanical properties, such as elasticity, plasticity, fracture strength, and other qualities. Thus, the deformation test from this point of view may be useful for studying the mechanical history of the earth's materials.

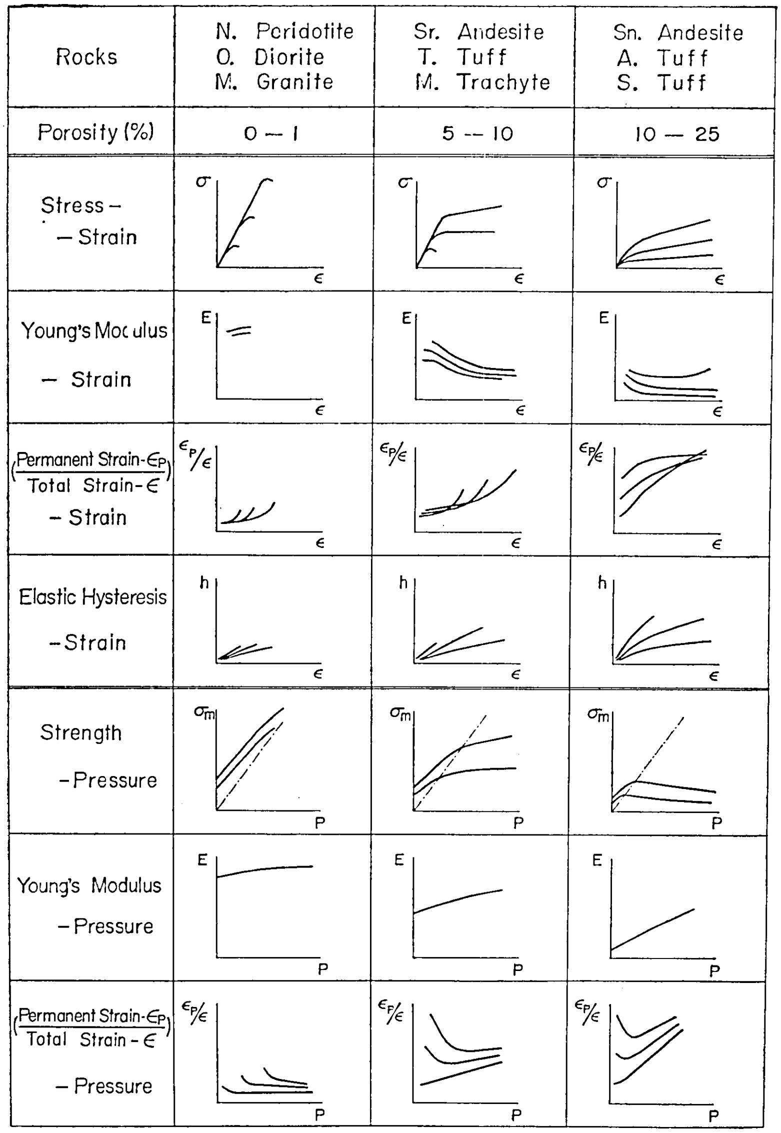

Fig. 19. Summary of experimental results.

9. Summary

By use of an indirect strain gage method, the stress-strain curves with cyclic loading branches were obtained for different types of rocks. Strength, elasticity, and plasticity were investigated as functions of the confining pressure. The rocks tested in the present experiment may be divided into three groups from their mechanical properties in this experiment. The mechanical properties in these rock groups are roughly summarized in Fig. 19, the range of porosity in these rocks being tabulated in this figure. From this result, it is clearly seen that the porosity is one of the most important factors for mechanical properties, with mineral compositions. It will be noted that the rocks in this figure are all silicate rocks, igneous or sedimentary. The marble seems to be different from these rock groups. The porosity of this marble is very small (abuot 0.15 percent), but this rock becomes remarkably ductile even under lower pressure and it seems to belong to the second group on the pressure effect. However, changes in mechanical properties by the increasing deformation of this rock are similar to the third group by reason of its high ductility. Thus, the mineral composition also may give an important effect to the mechanical behavior of rocks.

In this experiment, tested rocks numbered only ten and the applied confining pressure was too low to study the brittle-ductile transition of compact igneous rocks. This result should be refined by further experiments on many different types of rocks and under a wider range of pressure.

10. Acknowledgment

The writer wishes to thank the staff of the Science and Engineering Research Laboratory, Waseda University, especially Dr. G. Endō, for the use of the triaxial testing apparatus. The writer also wishes to express thanks to Dr. T. Matsuda for the petrographic description in this paper and to Dr. N. Yamakawa for valuable discussions.

Appendix: Petrographic descriptions of rocks

1. *Nabe-ishi peridotite—Nabe-ishi* is the trade name for the hornblende-peridotite quarried at Haruyama, Funahiki-machi, Fukushima prefecture. The rock is medium-grained and dark gray in color. It consists chiefly of hornblende which includes many grains of olivine. [hornblende (up to 1 cm in diameter): 74%, olivine (up to 1 mm in diameter): 25%].

2. *Orikabe dioite—Orikabe* is the trade name for the quartz diorite quarried at Orikabe, Murone-mura, Iwate prefecture. This rock is a gray, fine-grained pyroxene-hornblende-biotite diorite. The pyroxene is diopsidic and usually surrounded by green hornblende. [feldspar (2~5 mm): 67%, hornblende (1~3 mm): 10%, pyroxene (1~2 mm): 8%, biotite (5 mm): 7%, quartz: 5%, magnetite (1 mm): 3%].

3. *Mannari granite—Mannari* is the trade name for the pinkish granite quarried at Mannari, Okayama City. The rock is a coarse-grained biotite granite, with pink potash feldspar. [feldspar (2~7 mm): 46%, quartz (2~7 mm): 50%, biotite (2~3 mm): 4%].

4. *Mito marble*—This rock is a white calcite marble quarried at Oota, Ibaragi prefecture. It contains a little quartz (0.5~1 %). The grain diameter ranges from 0.5 mm to 2 mm.

5. *Shirochōba andesite—Shirochōba* is the trade name for the pyroxene andesite quarried at Manazuru, Kanagawa prefecture. The rock is light gray in color. Phenocrysts are plagioclase, pigeonite, augite, hypersthene and magnetite. The groundmass is pilotaxitic in texture and contains plagioclase, monoclinic pyroxene and magnetite. Quartz and tridymite are present in interspaces. [feldspar phenocryst (1 mm in length): 25%, pyroxene phenocryst (0.05 mm): 1%, pore: 5%, groundmass (chiefly plagioclase and glass): 69%].

6. *Tatsuyama tuff—Tatsuyama* is the trade name for the dacite (welded ?) pumice tuff quarried at Hōden, Hyōgo prefecture. The rock is compact and vaguely laminated. It is composed of devitrified pumice fragments and glass shards with phenocrysts of quartz and feldspar. [feldspar phenocryst (up to 1 mm in diameter): 3%, quartz (0.7 mm): 2%, iron saponite: 1%, lithic fragment: 7%, pore: 3%, devitrified matrix (chiefly feldspar): 84%].

7. *Mizuho trachyte—Mizuho* is the trade name for the trachyte obtained from a quarry at Tomioka, Gumma prefecture. The rock is massive and light brownish gray in color, with small spots of plagioclase phenocrysts. It is biotite- and quartz-bearing trachyte. The groundmass is holocrystalline and trachytic, and consists mainly of plagioclase. [feldspar (1 mm in diameter, partly altered): 12%, magnetite (0.1 mm): 4%, calcite (0.3 mm): 2%, iron saponite: 5%, pore (empty, rarely filled with clay minerals): 6%, groundmass (chiefly feldspar, 0.07~0.1 mm): 71%].

8. *Shinkomatsu andesite—Shinkomatsu* is the trade name for the pyroxene andesite (somma lava of Hakone volcano) quarried at Manazuru-machi, Kanagawa prefecture. The rock is very porous and is tarnished for minute hematite grains contained in groundmass. It contains plagioclase, monoclinic pyroxene and magnetite (hematite) both as phenocryst and fine-grained groundmass. [plagioclase phenocryst (1~1.5 mm in diameter): 24%, monoclinic pyroxene phenocrysts: 1%, groundmass: 59%, pore (1~3 mm in diameter): 16%].

9. *Ao-ishi tuff—Ao-ishi* is the trade name for the green tuff quarried at Izu-Nagaoka, Shizuoka prefecture. The rock is pale green and apparently massive, but is weakly and finely laminated on the polished surface. The tuff is pumiceous originally, now altered to aggregates of chlorite, albite, quartz, calcite, epidote and pyrite. [chlorite: 64%, plagioclase (a little quartz may be included): 30%, epidote: 6%, calcite: 2%, pyrite: 1%].

10. *Saku-ishi welded tuff—Saku-ishi* is the trade name for the andesitic welded tuff quarried at Oosawa, Nozawa-machi, Nagano prefecture. The rock is moderately welded and yellowish light gray in color, and weakly laminated. It contains phenocrysts of plagioclase, augite, hypersthene, and magnetite. The matrix is partly devitrified. Plagioclase and hypersthene are partly replaced by analcime and clay minerals. Small fragments of mudstone, sandstone, and andesite lapilli are included. [plagioclase (0.5~1.5

mm in diameter): 19%, pyroxene (0.3~1 mm): 2%, lithic fragments (2~20 mm) 6%, matrix: 68%, pore (0.2~1 mm): 5%].

---

23. 高封圧下の岩石の変形・破壊 (第2報) 弾性と塑性

地震研究所 茂 木 清 夫

前回にひきつづいて，各種岩石の高圧下の力学的諸性質を静的圧縮試験によつて調べた．今回は，変形測定法を改良することによつて，弾性領域から塑性領域にわたる，かなり広い変形範囲について，高精度の変形曲線を求めることができた．とくに，各変形段階で軸圧を0にもどすことにより，弾性変形部分と永久変形部分を分離して求めた．かくして，弾性変形，塑性変形，弾性率及び弾性履歴などが，変形の進行と共に変化する過程並びに静水圧との関係を求めることができた．さらに，強度と圧力の関係および破壊形式の脆性一延性遷移について考察した．
